



# Differential tolerance to summer stress conditions in two olive cultivars using the dendro-isotopic approach

S. Portarena<sup>a,b,\*</sup>, D. Farinelli<sup>c</sup>, F. Famiani<sup>c</sup>, N. Cinosi<sup>c</sup>, C. Traini<sup>c</sup>, N. Rezaei<sup>d</sup>, E. Brugnoli<sup>a</sup>

<sup>a</sup> Institute of Research on Terrestrial Ecosystems (IRET), National Research Council (CNR), Via G. Marconi 2, Porano, TR 05010, Italy

<sup>b</sup> National Biodiversity Future Center, Palermo 90133, Italy

<sup>c</sup> Department of Agricultural, Food, and Environmental Sciences (DSA3), University of Perugia, Via Borgo XX Giugno 74, Perugia 06121, Italy

<sup>d</sup> Institute of Research on Terrestrial Ecosystems (IRET), National Research Council (CNR), Via Madonna del Piano, 10, Sesto Fiorentino, FI 50019, Italy

## ARTICLE INFO

### Keywords:

*Olea europaea* L.  
Cultivar  
Tree rings  
Carbon isotope  
Oxygen isotope  
Intrinsic water-use efficiency

## ABSTRACT

In this study the interannual and seasonal dynamics of carbon and oxygen stable isotope composition ( $\delta^{13}\text{C}$ ,  $\delta^{18}\text{O}$ ), and the resulting intrinsic water use efficiency (iWUE) in xylem rings of *Olea europaea* L. were investigated. The study was conducted on two high-quality Italian olive cultivars (cv Moraiolo and cv Maurino), grown in central Italy, during the seasons 2020–2022. Variations in both C and O isotope compositions revealed seasonal patterns characterised by the lowest values within the transition from late to early wood rings and the highest values within the transition from early to late wood. The wider seasonal range of  $\delta^{13}\text{C}$ ,  $\delta^{18}\text{O}$  and iWUE observed in cv Moraiolo highlighted its ability to adapt to changing environmental conditions. During periods of summer stress, Moraiolo trees close their stomata to reduce transpiration rates, prioritising water conservation to sustain growth. In contrast, Maurino displayed less flexibility in vary its iWUE based on water availability, exhibiting limited responsiveness to environmental fluctuations. The relationship between ecophysiological traits and above-ground development of each cultivar was also discussed.

## 1. Introduction

Olive (*Olea europaea* L.) is a Mediterranean sclerophyll tree species known for its relatively high tolerance to drought (Fernández et al., 2013). In central and southern Italy, this crop holds significant importance, not only for its contributions to the region's distinctive landscapes but also for its fruit and oil production. Olive oil is renowned as a primary source of dietary fat in the Mediterranean diet and its production and consumption is steadily increasing due to its health benefits related to the balanced composition of fatty acids and antioxidant properties (Anselmi et al., 2022; Portarena et al., 2023). The Mediterranean region is characterized by severe summer conditions, including low rainfall, excessive heat load and high daily irradiance. Among the constituents of summer stress, drought and high temperatures are usually the most critical. Moreover, the Mediterranean area is highly vulnerable to the impacts of climate change, which presents a significant challenge for agriculture (Stocker et al., 2014). According to the Intergovernmental Panel on Climate Change (IPCC), climate change scenarios predict that the temperature will continue to rise and precipitation patterns will shift, leading to higher evaporative demand and reduced soil water

availability (Vinci et al., 2023a). Under such changing environmental conditions, the extent to which olive trees are sensitive to the combination of high summer temperatures and prolonged drought periods becomes crucial. This sensitivity plays a significant role in determining their physiological performance, growth, and, notably, fruit production (Rossi et al., 2013).

Among olive cultivars, there are significant genetic and phenotypic plasticity differences in responses to climate-related stresses (Bacelar et al., 2009; Brito et al., 2019). Despite the research efforts invested in studying the effect of climate change on olive crop yield and distribution, data that comprehensively assesses how different olive cultivars respond to climate variability are scarce.

Carbon and oxygen stable isotopes in tree-ring can be used to identify long-term adjustments in tree gas-exchange processes (Roden and Farquhar, 2012). In specific, carbon stable isotopes ( $\delta^{13}\text{C}$ ) have been used successfully to estimate the ratio of intercellular to atmospheric  $\text{CO}_2$  concentration ( $C_i/C_a$ ) which integrates the ratio of stomatal conductance to photosynthetic rates and, therefore, the intrinsic water-use efficiency (iWUE) of C3 plants (Farquhar et al., 1989; Cabrera-Bosquet et al., 2009; Di Matteo et al., 2010). On the other hand, oxygen stable

\* Correspondence to: IRET-CNR, Via G. Marconi 2, Porano, TR 05010, Italy.  
E-mail address: [silvia.portarena@cnr.it](mailto:silvia.portarena@cnr.it) (S. Portarena).

isotope composition ( $\delta^{18}\text{O}$ ) of organic carbon depends on  $^{18}\text{O}$  enrichment in leaf water during transpiration and provides insights into transpiration rates and water resource utilization (Scheidegger et al., 2000; Cabrera-Bosquet et al., 2011).

Until now, dendroecological investigations on olive trees have been limited in number due to the difficulty of accurately identifying annual tree-ring boundaries (Cherubini et al., 2003, 2013, 2014; Gea-Izquierdo et al., 2012; Rossi et al., 2013). In fact, in olive, annual rings do not always develop and, particularly under mild winter conditions and summer droughts, false rings or intra-annual density fluctuations may be formed (Cherubini et al., 2013; Battipaglia et al., 2016). Furthermore, the majority of studies involving  $\delta^{13}\text{C}$  and  $\delta^{18}\text{O}$  in tree rings are focused on inter-annual resolution, considering one measurement per annual ring, without distinguishing the time of wood formation during the growth season (Saurer et al., 2023).

Retrospective intra-annual tree ring stable isotope analyses, in addition to interannual analysis, may provide a more comprehensive understanding of plant physiological traits and their responses to seasonal variations.

To the best of our knowledge, for the first time, the present study analyzed the seasonal  $\delta^{13}\text{C}$ ,  $\delta^{18}\text{O}$  and derived intrinsic water-use efficiency (iWUE) variability within wood rings, with intra-annual resolution, showing seasonal response to environmental variables. These results were compared with agronomic and productive data during three years of growth. Young olive trees from two high quality Italian cultivars, Maurino and Moraiolo, grown in central Italy have been studied.

The main objectives of this study were to (i) determine, for each cultivar, the seasonal dynamics of intra-annual ring  $\delta^{13}\text{C}$ ,  $\delta^{18}\text{O}$  and the resulting iWUE; (ii) examine the relationships between tree ring  $\delta^{13}\text{C}$  and  $\delta^{18}\text{O}$  across the entire study period; (iii) understanding how stomatal control and photosynthetic activity may drive the variation of iWUE in relation to the agronomic/productive traits of each cultivar.

We hypothesized that trees from different cultivars exhibit different ecophysiological dynamics throughout the growing season, that can be reflected in their agronomic and productive responses.

## 2. Materials and methods

### 2.1. Orchard conditions, vegetative and productive measurements

The study was conducted between 2020 and 2022, on a rainfed, high-density olive orchard, located in central Italy ( $42^{\circ}59'23''$  N,  $12^{\circ}41'47''$  E, 260 m a.s.l.). The trees, obtained through self-rooting from cuttings, were initially grown in small pots ( $7 \times 7 \times 10$  cm). In the autumn of 2016, when the trees were 8 months old and had reached a height of 60 cm, they were transplanted into the orchard. The trees were trained as central leader bearing several lateral branches.

The orchard covered an area of 10,000 m<sup>2</sup>, with a tree density of 1000 trees per hectare. The spacing between individual trees was 2 m, and there was a distance of 5 m between rows. The sampling area covered approximately 500 m<sup>2</sup>.

The soil exhibited the following characteristics: medium-clay texture; pH:  $7.9 \pm 0.1$ ; organic matter content:  $1.4 \pm 0.1$  (%); active limestone:  $3.6 \pm 0.1$  (%); cation exchange capacity:  $25.6 \pm 0.5$  (meq/100 g); exchangeable potassium:  $273 \pm 43$  (mg/kg); and assimilable phosphorus:  $31.9 \pm 2.5$  (mg/kg) (Famiani et al., 2022).

In February 2018, winter low temperatures damaged the aerial parts of both Moraiolo and Maurino trees delaying their development. Two commonly grown cultivars in the region, Moraiolo and Maurino, were included in the trial. Moraiolo, native to central Italy, exhibits medium vegetative growth, medium-sized lanceolate leaves, small-sized fruit, high oil content, and produces high-quality oil during the mid to late season. Maurino, which has also originated from central Italy, is often utilized as a pollinator. It features medium vegetative growth, small elliptical leaves, small-sized fruit with medium-high oil content and produces high-quality oil during the early to mid-season.

Temperatures and precipitation data were obtained from a meteorological station located adjacent to the experimental field. This station recorded half-hourly averages of global radiation, air temperature, relative humidity, wind speed, and rainfall. Data were collected throughout the year, spanning from January 1st to December 31st for each of the three years (from 2020 to 2022).

Canopy height (H), canopy length along the row (L) and width (W), in the orthogonal direction with respect to the length, were manually measured at the end of the last vegetative season in 2022 for four trees of each cultivar. Since the plants were trained to form a continuous wall of vegetation, with plants closely spaced and trained using a single leader and multiple lateral branches, we modeled the canopy as a parallelepiped shape (Lodolini et al., 2023). The formula  $V = L \times W \times H$  was applied to determine the canopy volume (Anifantis et al., 2019).

The trunk diameter, taken at a height of 0.6 m from the ground, was measured in each winter, starting from December 2019 as the initial data point, for the same four trees of each cultivar. This measurement was used to calculate the trunk sectional area (TSA). The growth rate of the trunk section (GR%) was computed as follows:  $GR = \frac{TSA_n - TSA_{n-1}}{TSA_{n-1}} \times 100$ , where  $n$  represents the year of the tree section growth, and  $n-1$  denotes the previous year. This data collection process occurred from 2019 to 2022.

For the same eight sampling trees, four trees from the Moraiolo cultivar and four from the Maurino cultivar, the Leaf Area Index (LAI) was assessed at the end of July 2022, using manual methods. LAI, which represents the ratio of plant leaf area (m<sup>2</sup>) per unit of canopy cross-sectional area (m<sup>2</sup>), was determined by counting leaves at the intersection points of a grid set within the canopy. This procedure follows the methodology described by Farinelli et al. (2005).

The grid consisted of a horizontal bar with holes spaced 10 centimeters apart, where rods were inserted. During measurement, the bar was progressively moved at different distances from the trunk (e.g., 0 cm, 30 cm, 50 cm, and so on), until no leaves touched the rods within each hole. For each hole and at each distance from the trunk, the leaves in contact with the rods were counted.

Additionally, the leaf area of eight randomly selected leaves from each plant of each variety was measured using a scanner, with pixel values subsequently converted to cm<sup>2</sup> using the SigmaScan Pro 5.0 software. The total plant leaf area (m<sup>2</sup>) was calculated by multiplying the LAI by the canopy cross-sectional area (in square meters) for each tree.

To determine the yield per tree, olives, from each sampled tree, were manually harvested at the start of November 2022. The fruit's oil content, based on fresh weight, was assessed using an Infra Analyzer apparatus (Spectra Analyzer Zeutec, Rendsburg, Germany) according to Cinosi et al., (2023).

Yield efficiency was obtained as the ratio between olive/oil per tree and total tree leaf area.

### 2.2. Tree ring sampling, dendrochronological measurements, stable isotope analysis and iWUE calculation

Samples were collected from the same 6-year-old trees (2–3 m height, 5–8 cm stem diameter) used for vegetative and productive measurements.

At the end of July 2022, two disks were taken from the oldest branches of each tree, one for tree ring widths (RW) measurements and one for isotopic analyses. To measure the RW of 2022, a third disk was collected from the same trees at the end of March 2023. All disks were air-dried and polished using sandpaper with varying grain sizes to enhance cell visibility in the cross-sectional view and to delineate the tree-ring boundaries.

The RW was measured at 0.01 mm resolution using a LINTAB (Rinntech, Heidelberg, Germany) equipped with a Leica MS5 stereoscope (Leica Microsystems, Wetzlar, Germany) and TSAPWin software

(Frank Rinn, Heidelberg, Germany). Due to the asymmetric cambial growth, the measurements were taken along three radii per disk. The three RW series per disk were averaged after visual cross dating to identify common marker years and RW patterns (Stokes and Smiley, 1968). To validate the accuracy of cross-dating and measurements, the dplR package (Bunn, 2008), within the R environment, was employed.

A sliding microtome (GSL1 microtome, WSL) was employed to cut the rings into approximately 10  $\mu\text{m}$  tangential slices, spanning the period from the start of earlywood formation in 2020 to July 2022. Detailed records were maintained to determine the specific growth ring to which each sample belonged, as well as its position within the earlywood (EW) or latewood (LW). It's important to note that due to the ambiguous nature of olive tree boundaries (Cherubini et al., 2003), there may be some margins of error in precisely identifying the transition from one year to the next.

In the initial phase, each consecutive 10  $\mu\text{m}$  wood sample collected from a growth ring was analysed. However, contiguous samples, particularly within the early wood, exhibited minimal variations in their isotopic values. Consequently, the resolution was adjusted and reduced to align with the RW. This adjustment means that the analyzed samples are still derived from 10  $\mu\text{m}$  sections, but not every individual contiguous sample was subjected to analysis.

$\delta^{13}\text{C}$  and  $\delta^{18}\text{O}$  analyses were conducted on the individual intra-annual tangential wood ring slices, obtained from the lowest unsanded cross-section.

Analyses of the  $^{13}\text{C}/^{12}\text{C}$  and  $^{18}\text{O}/^{16}\text{O}$  isotope ratios were performed using an isotope ratio mass spectrometer (IRMS) (Isoprime, GV, Cheadle, UK) connected to an elemental analyser (NA1500, Carlo Erba, Milan, Italy) and to a pyrolysis system (Euro Pyr-OH, Euro Vector Instruments & Software, Milan, Italy).

An aliquot of about 0.5 mg wood dry matter was collected to perform both isotope analyses.

The isotopic compositions were scale-normalised with the IAEA international standards and are expressed as  $\delta$  notation according to the following expression:

$$\delta (\text{‰}) = (R_s - R_{\text{std}})/R_{\text{std}} \times 1000, \quad (1)$$

where  $R_s$  is the isotope ratio of the sample and  $R_{\text{std}}$  is the isotope ratio of the international standard.

L-glutamic acid USGS 40 (IAEA – International Atomic Energy Agency, Vienna, Austria,  $\delta^{13}\text{C} = -26.2\text{‰}$ ), NBS-22 fuel oil (IAEA,  $\delta^{13}\text{C} = -30.03\text{‰}$ ) and IAEA-CH6 sucrose ( $\delta^{13}\text{C} = -27.5\text{‰}$ ) were used for the scale normalization of the measured  $\delta^{13}\text{C}$  values to the Vienna-Pee Dee Belemnite (VPDB) international standard. IAEA-CH6 Sucrose ( $\delta^{18}\text{O} = +36.4\text{‰}$ ), IAEA-601 benzoic acid ( $\delta^{18}\text{O} = 23.14\text{‰}$ ) were used for scale normalization of measured  $\delta^{18}\text{O}$  values to the VSMOW scale.

Each single tree ring wood samples was measured in duplicate and the mean values were considered. For  $\delta^{13}\text{C}$ , the standard deviation (SD) of replicate measurements for each standard and sample was 0.1‰ and  $\pm 0.3\text{‰}$  respectively. For  $\delta^{18}\text{O}$  the SD of replicate measurements for each standard and sample was  $\pm 0.3\text{‰}$  and  $\pm 0.5\text{‰}$ . Possible changes in analytical conditions within a run were corrected using USGS 40, NBS-22 and IAEA-CH6 for the  $\delta^{13}\text{C}$  measurements and IAEA-601 and IAEA-CH6 sucrose for  $\delta^{18}\text{O}$ .

The  $\Delta^{13}\text{C}$  (carbon isotopic discrimination) of the wood tree rings was calculated as

$$\Delta^{13}\text{C} = (\delta^{13}\text{C}_{\text{air}} - \delta^{13}\text{C}_{\text{plant}})/(1 - \delta^{13}\text{C}_{\text{plant}}) \quad (2)$$

following Farquhar et al. (1982) and using published values for air  $\delta^{13}\text{C}$  relative to each year to take into account of the so called Suess effect (<https://gml.noaa.gov/dv/iadv/graph.php?code=MLO&program=ccgg&type=fi>).

$\Delta^{13}\text{C}$  is related to the  $C_i$  over  $C_a$  ratio by the following equation:

$$\Delta^{13}\text{C} = a + (b-a) \times (C_i/C_a) \quad (3)$$

where  $a$  is the discrimination against  $^{13}\text{C}$  during  $\text{CO}_2$  diffusion through stomata ( $a = 4.4\text{‰}$ ) and  $b$  is the discrimination associated with carboxylation ( $b = 27\text{‰}$ ) (Farquhar et al., 1982; Brugnoli and Farquhar, 2000);  $C_i$  and  $C_a$  are the  $\text{CO}_2$  concentrations in the intercellular air space of the leaves and in the atmosphere, respectively.

$C_a$  values were collected from NOAA as described above.

$C_i$  can be obtained based on Eqs. (2) and (3).

The iWUE is the ratio of net photosynthetic  $\text{CO}_2$  assimilation rate (A) to stomatal conductance ( $g_s$ ) (Ehleringer and Monson, 1993) and was calculated as:

$$\text{iWUE} = A/g_s = C_a \times [(1 - C_i/C_a)/1.6] = C_a \times [1 - (\Delta a)/(b-a)]/1.6 \quad (4)$$

where 1.6 is the ratio of binary diffusivities of water and  $\text{CO}_2$  in air.

### 2.3. Statistical analysis

For the agronomic, productive, isotopic/derived variables ( $\delta^{13}\text{C}$ ,  $\delta^{18}\text{O}$  and iWUE) and RW, the mean values and standard errors (SE) were calculated over four plants per cultivar.

The t-test and Post Hoc Fisher comparison test were used to determine whether there was significant difference between cultivar in the mean values of the measured variables.

The Granger Causality test was performed for detecting differences between cultivars in iWUE time series.

The Pearson coefficient ( $r$ ) was computed between RW and climatic values and between  $\delta^{13}\text{C}$  and  $\delta^{18}\text{O}$  values to check for the existence of a correlation between the selected variables. The linear equation relating the  $\delta^{13}\text{C}$  and  $\delta^{18}\text{O}$  values was also determined. Analysis of covariance (ANCOVA) and Post Hoc Fisher multiple comparison test were used to determine whether there was significant difference among the slopes.

The statistical significance of all the analyses was fixed at p-value  $\leq 0.05$ .

Statistical analyses were performed using Statistica v8 (Stat-Soft Italia srl, Padua, Italy) and R (R Development Core Team, 2018).

## 3. Results

### 3.1. Weather condition, vegetative and productive measurements

Throughout the studied years, the summer months were consistently marked by extended periods of exposure to temperatures within the range of 35–40°C. (Fig. 1).

In 2021, the month of September also experienced maximum temperatures exceeding 32°C. Moreover, in 2022, elevated maximum temperatures exceeding 33°C were also observed in May and September. The mean maximum temperature, calculated for the same summer months, exhibited an upward trend from 2020 to 2022, with values of 36.5°C, 37.5°C, and 38.8°C, respectively. A similar pattern was observed for minimum temperatures, averaged within the June to August summer months trimester, with values of 23.5°C, 24.7°C, and 26.3°C for 2020, 2021, and 2022.

In 2020 and 2022, both monthly maximum and minimum temperatures showed an increase from February to July, followed by a decrease until December. In contrast, in 2021, the maximum temperatures reached their peak values in August, averaging 38.7°C during that month.

In 2021 spring (April) frosting temperatures damaged the inflorescences, causing a complete loss of yield in both the considered cultivars (Moraiole and Maurino).

The total annual rainfall amounted to 785 mm, 551 mm, and 705 mm for the years 2020, 2021, and 2022 (Fig. 1). During the summer months, from June to August, rainfall levels were 212 mm, 24 mm, and 109 mm in 2020, 2021, and 2022, respectively. However, between the fruit-setting and olive harvest period, spanning from June to October, the total rainfall reached 399 mm, 106 mm, and 267 mm in 2020, 2021,

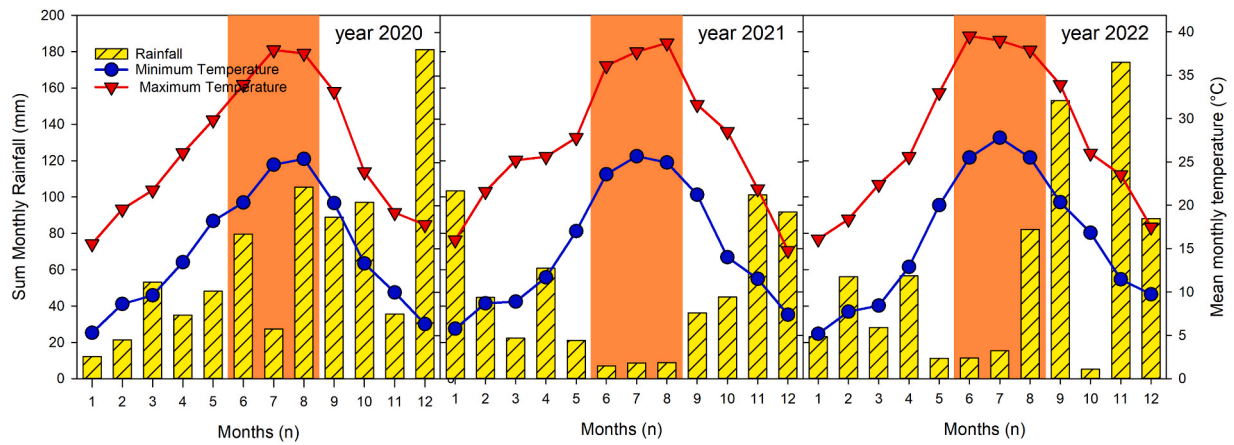


Fig. 1. Climatic data (sum monthly rainfall, mean of minimum and maximum monthly temperatures) recorded in the experimental orchard from 2020 to 2022. The orange column represents the summer months.

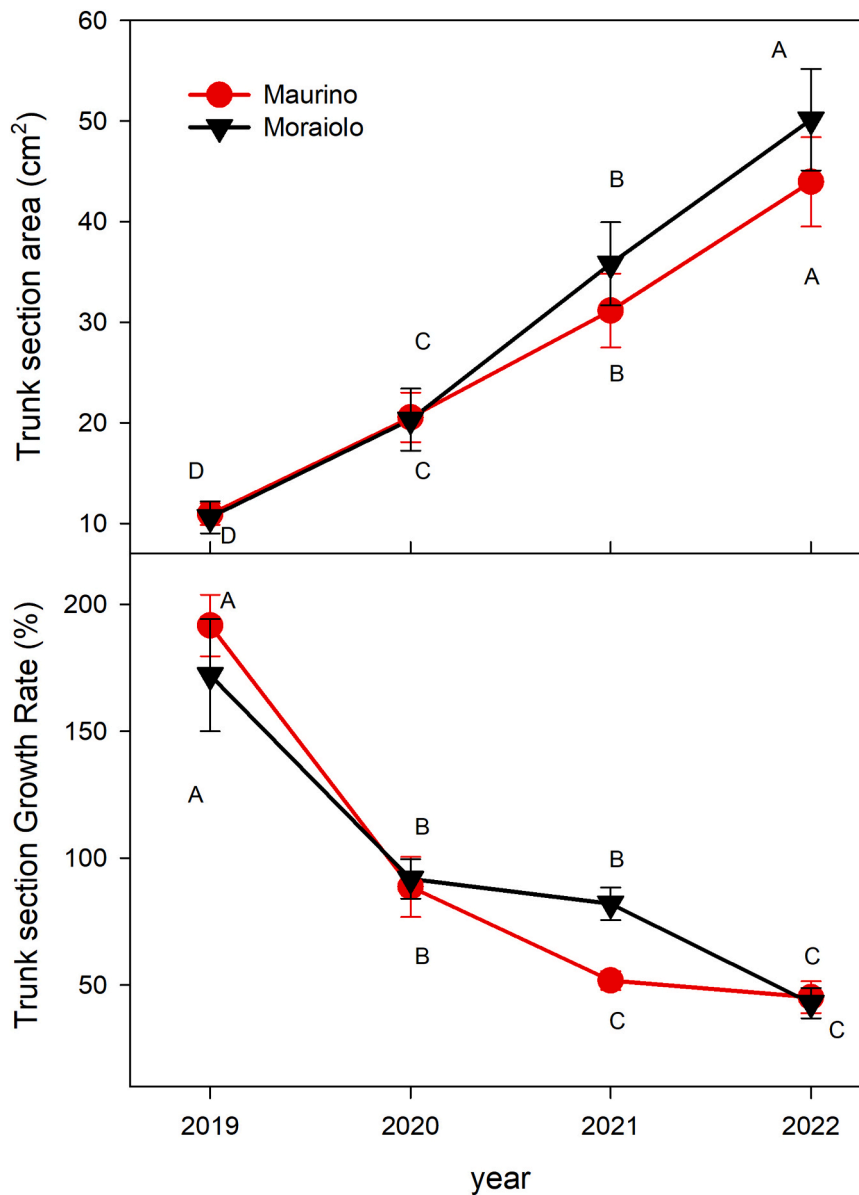


Fig. 2. Trunk section area at the top; Trunk section Growth Rate at the bottom. Data are reported of mean  $\pm$  SE. Means accompanied by different letters are statistically different for  $p < 0.05$ .

and 2022, respectively.

In both cultivar, the trunk section area increased from 2019 to 2022. Although the differences between cultivars were not statistically significant, in the last two sampling years Moraiolo exhibited higher values for trunk section area (Fig. 2).

In Moraiolo the trunk section area increased from and 10.6–50.1 cm<sup>2</sup>; in Maurino it increased from 10.9 cm<sup>2</sup> to 44.0 cm<sup>2</sup> (Fig. 2). On the other hand, the trunk section growing rate resulted to be different between the two cultivars. In specific, Maurino showed a significant and constant decreasing trend of growing rate over the studied years, from 192% to 45%; while Moraiolo, even showing a decreasing trunk section growth rate, had a growing rate not statistically different between 2020 and 2021, respectively 91.8% and 82.0% (Fig. 2).

The canopy volume, leaf area index and yield efficiency are reported in Fig. 3.

Yield per tree was of 2.9, 0.0 and 4.6 kg for Maurino and 2.6, 0.0 and 2.5 kg for Moraiolo, in the years 2020, 2021 and 2022, respectively, and as a result the cumulated yield per tree was 7.5 kg for Maurino and 5.1 kg for Moraiolo. The oil content on fresh weight in the fruits was

21.4 and 19.6 in Maurino and 19.6 and 23.0 in Moraiolo, in the years 2020 and 2022, respectively.

The canopy volume resulted not statistically different between the two cultivars, with averaged values of 4.8 m<sup>3</sup> and 4.1 m<sup>3</sup> respectively in Maurino and Moraiolo (Fig. 3). However, the LAI was notably higher in Maurino (6.4) compared to Moraiolo (5.1). The fruit oil content was higher in Moraiolo (Fig. 3).

### 3.2. Dendrochronological measurements, stable isotope analyses and *i*WUE calculation

The temporal trends in RW for the two cultivars are shown in Fig. 4.

The branches of the sampled cultivars covered a five-year period, spanning from 2018 to 2022. In both chronologies, the expressed population signal (EPS) exceeded the critical value of 0.85, indicating a significant common signal.

A significant correlation between RW of Moraiolo and Maurino was observed (R=0.79, P-value < 0.001).

In Moraiolo significant correlations were identified between RW and

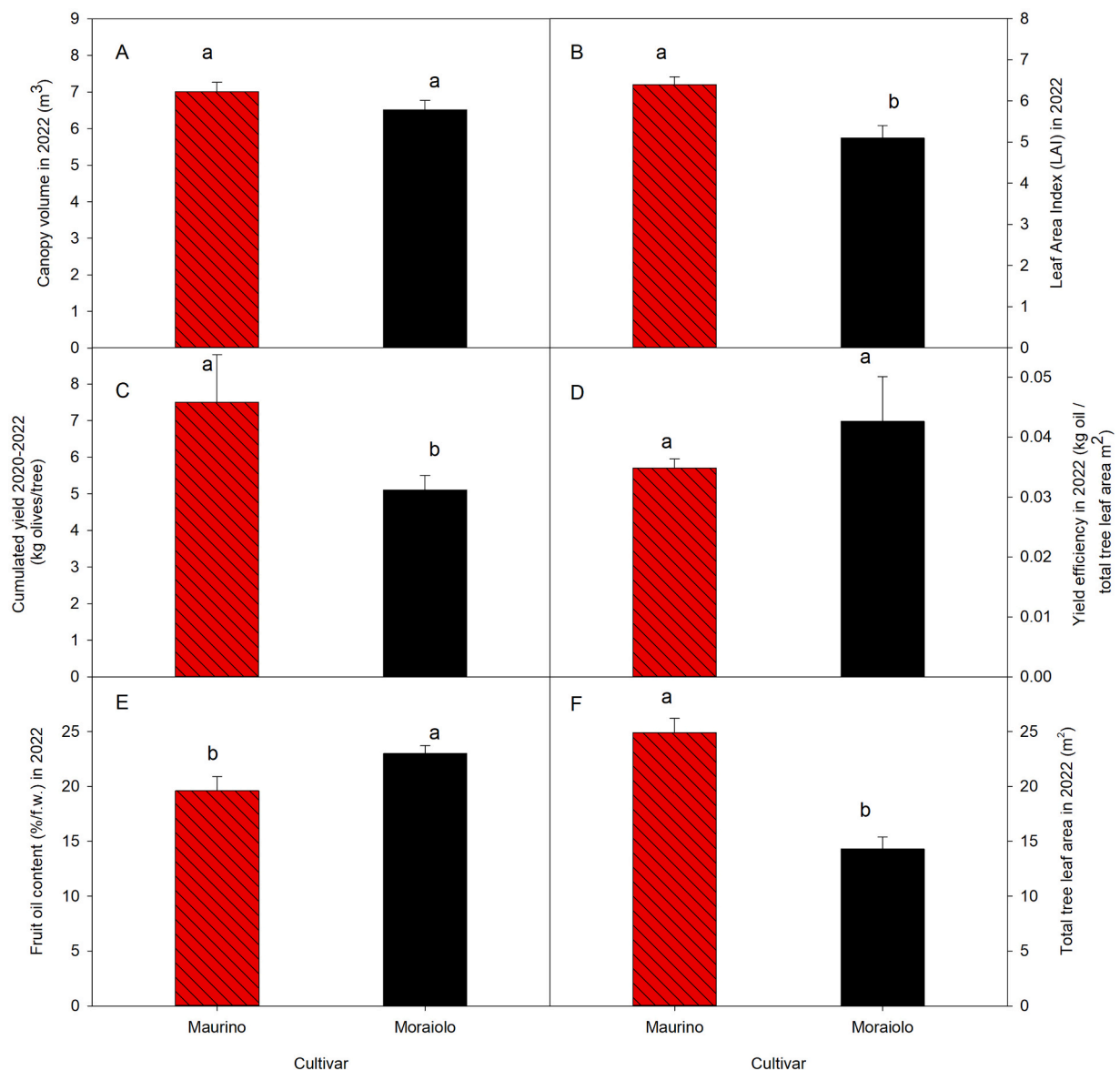


**Fig. 3.** Canopy volume (A), Leaf Area Index (LAI) (B); Cumulate Yield 2020–2022 (C); Yield efficiency in 2022 as ratio between oil per tree and total tree leaf area (D); Fruit oil content in 2022 (E); Total tree leaf area in 2022 (F). Data are reported as mean  $\pm$  SE. Means accompanied by different letters are statistically different for  $p < 0.05$ .

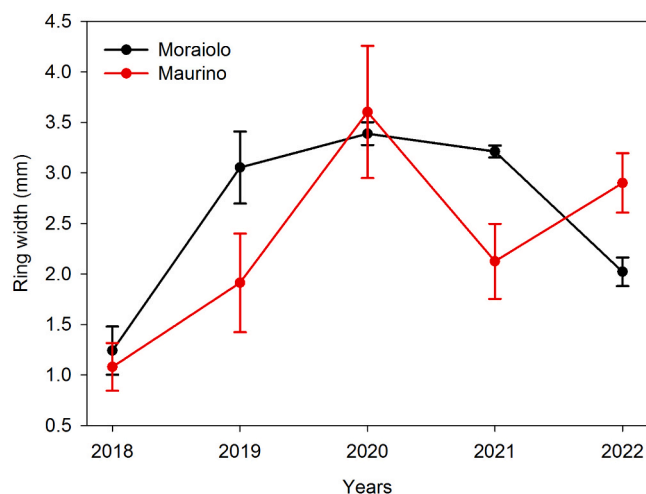


Fig. 4. Ring width (mm) temporal trends reported as averages over the four sampled trees per cultivar: Moraiolo (black line), Maurino (red line). Bars represent the standard errors.

temperature as well as precipitation. Specifically, RW exhibited negative correlations with the maximum temperature in June and July ( $r = -0.82$  and  $r = -0.81$ ,  $P < 0.05$ ) and it was positively influenced from the May precipitation ( $r = 0.72$ ,  $P < 0.05$ ). No significant correlations were found in Maurino.

The intra-annual patterns of wood rings  $\delta^{13}\text{C}$  and  $\delta^{18}\text{O}$  for the period 2020–2022 are shown in Fig. 5.

A seasonal pattern can be observed in both cultivars (Fig. 5). The lowest  $\delta^{13}\text{C}$  values were observed near the transition from LW to EW, where most likely the annual ring transition occurred. Subsequently,  $\delta^{13}\text{C}$  values steadily increased in the EW, reaching their peak at the transition from EW to LW, referred to as the seasonal ring transition. In the LW,  $\delta^{13}\text{C}$  values gradually decreased. Furthermore, in all three years, the rise in  $\delta^{13}\text{C}$  values in the EW was characterized by a slight dip just before reaching the maximum  $\delta^{13}\text{C}$  value, resulting in the presence of a trough before the  $\delta^{13}\text{C}$  peak.

In both 2020 and 2021, significant differences between the cultivars were observed in the LW  $\delta^{13}\text{C}$  values, with average values of  $-26.2\text{‰}$  and  $-24.33\text{‰}$  for Moraiolo, and  $-25.7\text{‰}$  and  $-25.8\text{‰}$  for Maurino, for the two years respectively. Similarly, in the same years, significant differences between cultivars were evident in the EW  $\delta^{13}\text{C}$ , with average values of  $-26.0\text{‰}$  and  $-24.9\text{‰}$  for Moraiolo, and  $-25.7\text{‰}$  and  $-25.1\text{‰}$  for Maurino, in the two years respectively.

In 2022, there were no significant differences between cultivars in the averaged values of both LW and EW  $\delta^{13}\text{C}$ . However, the most pronounced seasonal variation in  $\delta^{13}\text{C}$  values occurred in Moraiolo during 2021, with a range of 4.1‰. In contrast, during the same year, Maurino displayed a more limited  $\delta^{13}\text{C}$  seasonal range of variation of 2.2‰.

The  $\delta^{18}\text{O}$  values were consistently higher in Maurino compared to Moraiolo across the entire study period.

Specifically, in 2020 and 2021, significant differences between cultivars were detected in the LW  $\delta^{18}\text{O}$  values, with average values of 24.1‰ and 24.9‰ for Moraiolo and 25.9‰ and 26.5‰ for Maurino, in the two years respectively.

Significant differences were also observed between the two cultivars in EW  $\delta^{18}\text{O}$  with averaged values of 25.4‰ and 24.3‰ and 25.3‰ for Moraiolo and 27.3‰, 25.3‰ and 26.7‰ for Maurino in 2020, 2021 and 2022, respectively.

Correlations between  $\delta^{13}\text{C}$  and  $\delta^{18}\text{O}$  in the two cultivars are plotted in Fig. 6.

The  $\delta^{13}\text{C}$  and  $\delta^{18}\text{O}$  were significantly and positively correlated in both cultivars (Fig. 6).

Additionally, significant differences between cultivars were found in

the slopes of the two linear equations.

Maurino exhibited the steepest slope, with an increase of approximately 0.82‰ in  $\delta^{18}\text{O}$  for every 1‰ increase in  $\delta^{13}\text{C}$ , and a correlation coefficient of  $r = 0.43$  ( $p < 0.05$ ).

In contrast, Moraiolo displayed a shallower slope of 0.48‰ in  $\delta^{18}\text{O}$  for every 1‰ increase in  $\delta^{13}\text{C}$ , and a correlation coefficient of  $r = 0.42$  ( $p < 0.05$ ).

In both cultivars, the total range of  $\delta^{13}\text{C}$  variation resulted lower than that of  $\delta^{18}\text{O}$ . In specific, in Moraiolo the isotopic ranges of variation were approximately 4‰ for  $\delta^{13}\text{C}$  and 6‰ for  $\delta^{18}\text{O}$ . Lower ranges of variation were observed in Maurino, approximately 2.2‰ for  $\delta^{13}\text{C}$  and 4‰ for  $\delta^{18}\text{O}$ .

Wood ring  $\delta^{13}\text{C}$  values have been used as indicators of iWUE (Fig. 7). This is because of the linear relationship between the ratio of intercellular to atmospheric  $\text{CO}_2$  concentrations ( $C_i/C_a$ ) and  $\delta^{13}\text{C}$  (Farquhar et al., 1982).

A seasonal pattern was evident in both cultivars (Fig. 7). The lowest iWUE values were observed near the annual ring transition. The iWUE values steadily increased in the EW to reach a maximum at the seasonal ring transition. In the LW, the  $\delta^{13}\text{C}$  value steadily decreased. The Granger Causality test identified significant differences in iWUE time series between the two cultivars.

The greatest seasonal variation in iWUE was found in Moraiolo over the 2021 with a range of  $47 \mu\text{mol CO}_2 \cdot \text{mol}^{-1} \text{H}_2\text{O}$ . During the same year, Maurino exhibited a iWUE seasonal range of variation of  $25 \mu\text{mol CO}_2 \cdot \text{mol}^{-1} \text{H}_2\text{O}$ .

#### 4. Discussion

Different growth patterns and ecophysiological behaviour were evidenced in two distinct olive tree cultivars, Moraiolo and Maurino, grown in central Italy. The two cultivars showed distinct responses to environmental parameters such as summer high temperature and precipitation patterns.

The observed increasing trend in mean annual temperatures recorded in the experimental orchard aligned with the findings reported by Vinci et al. (2023b) in the Umbria region, particularly noting the occurrence of very hot summers. Vinci et al. (2023a) and Di Lena et al. (2022) have both highlighted a significant upward trend in evapotranspiration in Central Italy. This is reflected in increasing summer stress in crops and, specifically in olive orchards.

Although its sclerophyllic characteristics, the olive crop is especially sensitive to water stress along the whole vegetative-fruiting season. However, in central Italy, there are three main critical periods: full-bloom/fruit-set, the initial phase of fruit growth (mainly by cell multiplication) and the phase of fruit growth (by cell extension) after pit-hardening, during which oil is accumulated (pit-hardening in central Italy occurs in the second half of July). These phases represent key stages for olive tree growth and productivity, especially for fruit development when water availability and temperatures play a crucial role in ensuring optimal yield and oil production (Branquinho et al., 2021).

In central Italy, the most critical period for olive productivity has been identified as the oil accumulation period, as highlighted by Finelli and Tombesi (2015). This phase is characterized by high temperatures and limited water availability (Fig. 1).

In 2022, the sixth year after planting, the two cultivars did not exhibit significant differences in terms of canopy volume. The observed LAI values resulted higher than those reported by Lodolini et al. (2023), in an older and denser orchard. The higher LAI observed in Maurino indicated that this cultivar had a denser canopy with a total greater leaf surface area, influencing light interception, photosynthetic activity and transpiration rates. This characteristic could have contributed to the overall productivity, including greater yield per tree.

Despite differences in LAI, yield efficiency was not found to be significantly different between the two cultivars. This implies that both Moraiolo and Maurino had similar overall efficiency in converting their

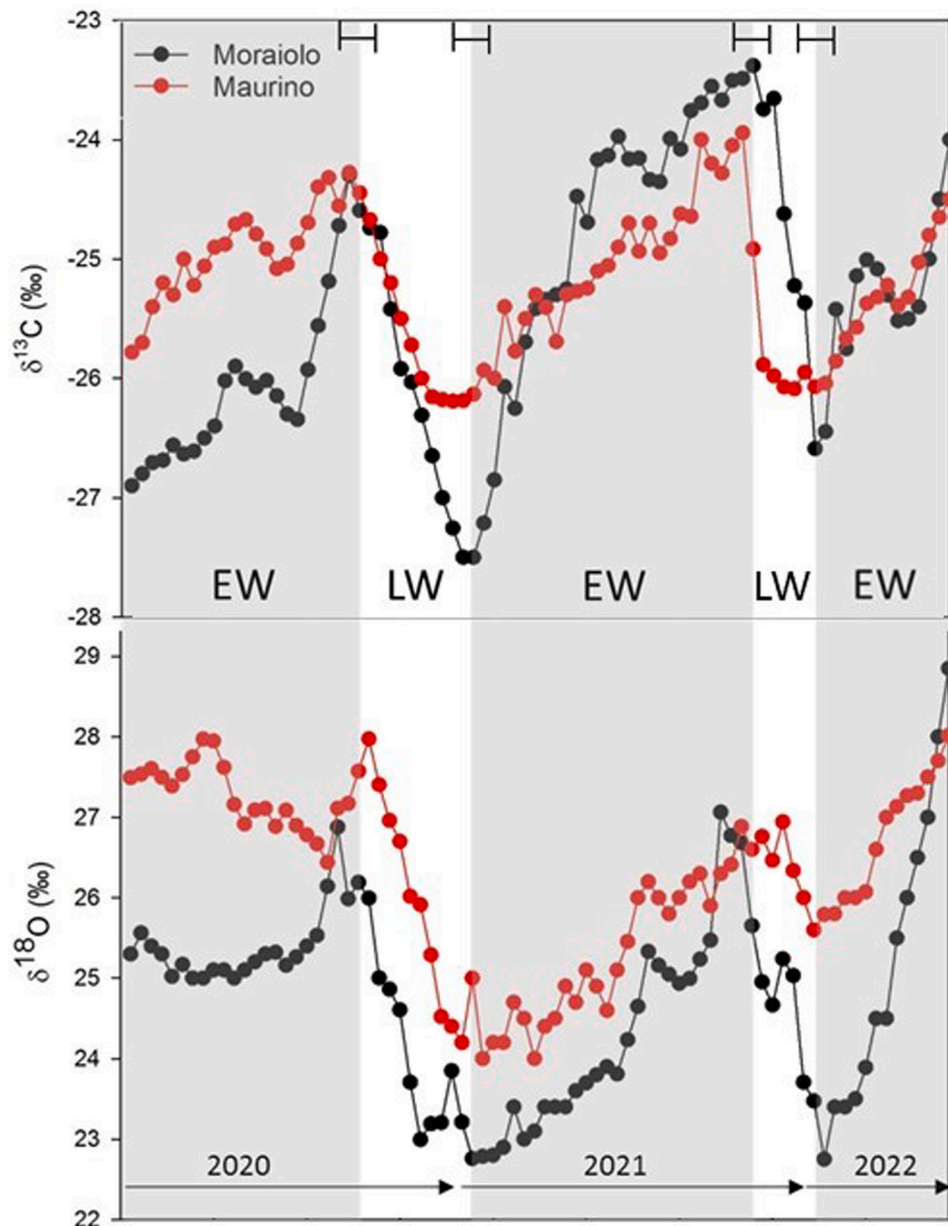


**Fig. 5.**  $\delta^{13}\text{C}$  (above) and  $\delta^{18}\text{O}$  (below) intra-annual pattern across the tree rings of *Olea europaea* L. from Moraiolo (black symbols) and Maurino (red symbols) cultivars, and ring boundaries (earlywood, EW, shaded background; latewood, LW, white background). Standard error bars for each ring were omitted for a clear representation. The uncertainty on the position of EW and LW boundaries is shown as horizontal error bars.

canopy structure into fruit yield.

Interestingly, the fruit oil content was higher in Moraiolo, indicating that while Maurino may have had a higher overall yield, Moraiolo had a distinct advantage in terms of oil production. Maurino tended to undergo a more rapid decrease in trunk section growth over time, indicating more stable stem structure with allocation of resources preferentially towards the uppermost part of the tree (Fig. 2 and Fig. 3). On the other hand, Moraiolo maintains a relatively stable trunk section growth rate, potentially indicating a more balanced allocation of resources between vegetative and reproductive growth over the years (Fig. 2 and Fig. 3).

The sensitivity of RW to climate parameters differed between the two cultivars. In Moraiolo, the negative correlation between RW and temperatures in June and July suggested that the cambial activity was constrained by high temperatures that worsen water deficit. Elevated temperatures contribute to increased evapotranspiration and soil water

losses (Battipaglia et al., 2010). The positive correlation with May precipitation underscores the significance of water availability during the spring season. Conversely, the absence of a significant relationship between climate data and RW in Maurino suggests that cambial cell activity in this cultivar may be less responsive to seasonal climate changes. The notably lower RW values recorded in Maurino during 2021 could potentially be attributed to the drought stress experienced by this cultivar during the summer (Fig. 4 and Fig. 1).

The intra-annual variability of stable isotope fractionation in tree rings reflects the interaction between intra-seasonal climate fluctuation and the plant's physiological responses. In fact, the seasonal climate variability might have caused variations in plant water source, atmospheric humidity, evaporative demand, photosynthesis and transpiration processes, with effects on both the isotopic compositions of current assimilates and then of synthesized wood rings. Of course, differences in the source of carbon for wood synthesis may also cause variation in the

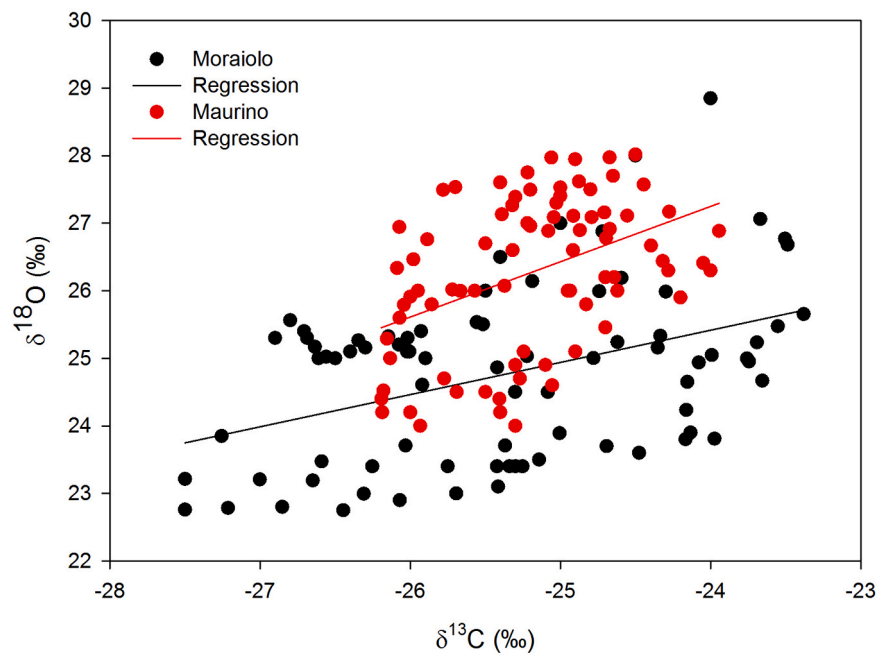


**Fig. 6.**  $\delta^{18}\text{O}$  -  $\delta^{13}\text{C}$  relationships in Moraiolo (black symbols,  $\delta^{18}\text{O} = 0.48 \delta^{13}\text{C} + 37.0$ ;  $r = 0.42$ ,  $p < 0.05$ ) and Maurino (red symbols,  $\delta^{18}\text{O} = 0.82 \delta^{13}\text{C} + 46.9$ ;  $r = 0.43$ ,  $p < 0.05$ ). Each data point represents a wood sample from a slide.

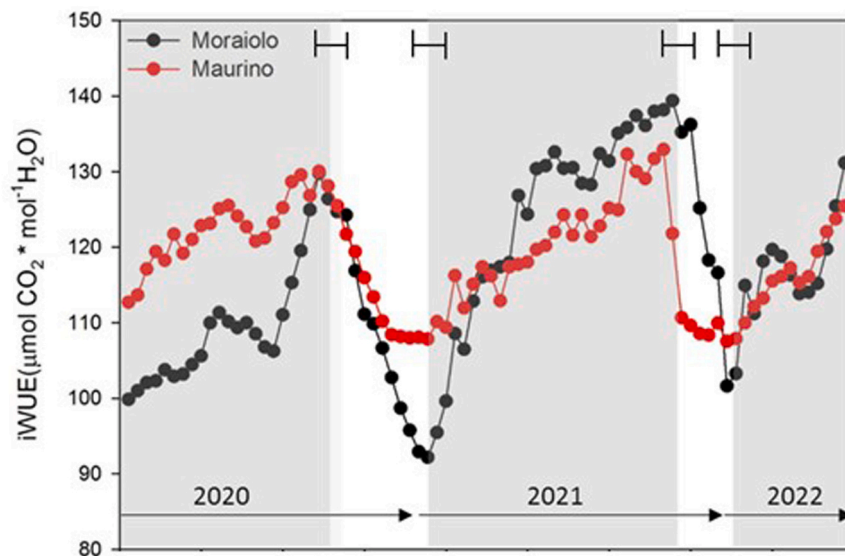


**Fig. 7.** iWUE intra-annual pattern across the tree ring sections of *Olea europaea* L. from Moraiolo (black symbols) and Maurino (red symbols) cultivars, and ring boundaries (earlywood, EW, shaded background; latewood, LW, white background). Standard error bars for each ring were omitted for a clear representation. The uncertainty on the position of EW and LW boundaries is shown as horizontal error bars.

isotopic signatures withing the same annual ring.

Olive tree, as an evergreen species, can continue photosynthesis even during the winter, ensuring a year-round supply of sugars through active photosynthesis. This ongoing photosynthesis supports wood synthesis with a continuous influx of current assimilates throughout the yearly growing season (Gessler et al., 2014). Cambial activity is continuous throughout the year, exhibiting a reduced rate during winter and the hotter summer period (Lipshitz and Lev-Yadun, 1986).

The development of earlywood and latewood in olive trees is influenced by various factors, including local climate conditions and cultivar characteristics. Our observations indicated that the branch disk collected in March 2023 had recently entered the earlywood stage. Conversely, sections obtained from the same trees collected in October

displayed the start of latewood formation (data not shown). This evidence suggests that earlywood initiation occurs in early spring, while latewood formation begins in the fall, coinciding with the conclusion of fruit development.

The general increasing temperatures and decreasing amount of rain, from spring to summer, may lead to a decrease of  $C_i/C_a$  during the EW formation and then to increasing values of  $\delta^{13}\text{C}$ . A low  $C_i/C_a$  ratio implies that stomata undergo partial stomatal closure, resulting in reduced  $g_s$ . In such conditions, the trees might still photosynthesize, but at a lower rate. Hence, the  $\delta^{13}\text{C}$  values in plant tissues would increase reflecting a decreased discrimination and a consequent greater fixation of  $^{13}\text{C}$ -enriched atmospheric  $\text{CO}_2$ .

Conversely, the wetter condition from autumn to winter led to



increasing  $C_i/C_a$  values with a decrease of  $\delta^{13}C$  in during the LW formation (Brugnoli and Farquhar, 2000; Farquhar et al., 1989). A high  $C_i/C_a$  ratio implies that  $g_s$  is not limiting photosynthesis, allowing relatively high photosynthetic  $CO_2$  uptake. Accordingly,  $\delta^{13}C$  values in the plant tissue tend to be lower, reflecting greater discrimination and a lower fixation of  $^{13}C$   $CO_2$ .

The lowest  $\delta^{13}C$  values were observed at the annual ring transitions, corresponding to wood formed towards the end of winter. As we move into the EW, there is a gradual increase in the  $\delta^{13}C$  value. The  $\delta^{13}C$  value reached a maximum at the seasonal ring transition, most likely corresponding to the wood formed during the transition period from summer to autumn.

The presence of a trough in the  $\delta^{13}C$ , just before reaching the maximum value may be associated with the onset of a brief period of drought stress: prolonged periods of drought during the growing season can lead to a reduction in photosynthesis, increase in  $C_i/C_a$ , which may result in lower  $\delta^{13}C$  values (Farquhar et al., 1989). Trees may temporarily close their stomata to conserve water during drought, reducing the photosynthetic activity, which in turn lowers the  $\delta^{13}C$  values of current assimilates and then wood rings (Cinosi et al., 2024).

Another factor contributing to the decline in  $^{13}C$  in the mid-section of EW may be associated with carbon isotope partitioning between different tree organs (Helle and Schleser, 2004). We hypothesize that the lignification of fruit endosperm, which takes place in early July, could lead to starch depletion in bark and xylem tissues, consequently resulting in a  $\delta^{13}C$ -depleted wood (Drossopoulos and Niavis, 1988). However, transition from vegetative to flowering stage might also influence leaf physiology, photosynthesis and, especially source-sink relations, with flowers and then fruit set becoming a relatively strong sink.

Differences in  $\delta^{13}C$  range of variations observed between the two cultivars might reflected their distinct responses to seasonal variations in both stomatal and biochemical processes.

During the initial winter season (December 2020-February 2021), the maximum amount of precipitation was recorded. Moraiolo exhibited the lowest mean  $\delta^{13}C$  values at the annual ring boundary for 2020/2021 ( $-27.5\%$ ). In contrast, the subsequent summer of 2021, characterized by relatively lower precipitation and higher temperatures, led to a significant enrichment in  $\delta^{13}C$  values. Moraiolo displayed the highest mean  $\delta^{13}C$  values during the summer/autumn transition of 2021/2022 ( $-23.4\%$ ).

During the same period of wood formation, Maurino exhibited narrower ranges of  $\delta^{13}C$  variations, with values spanning from  $-26.2\%$  to  $-23.9\%$  for the annual and the seasonal ring boundaries, respectively.

In the season 2022 the  $\delta^{13}C$  variation was less pronounced in both cultivars depending on the climatic conditions during plant growth and to the constraint of limited wood sampling time that occurred in July 2022.

The  $\delta^{18}O$  value in plant material reflected various factors, including the source of water, the evaporative enrichment of  $^{18}O$  in leaf water due to transpiration, and the biochemical processes occurring during the formation of organic matter and metabolism (Battipaglia et al., 2013; Saurer et al., 1997; Tene et al., 2011).

It is important to underline that our assumption is that the  $\delta^{18}O$  patterns observed in the two cultivars are not attributed to hydrological or pedological variations among the sampled trees. Both Moraiolo and Maurino olive trees were situated within a confined area (approximately 500 m<sup>2</sup>), characterized by identical soil composition (refer to Orchard Conditions, Vegetative, and Productive Measurements section). Furthermore, previous observations have verified the absence of a groundwater table and have established that the primary water source for the area is infiltration from local rainfall.

In the years 2021 and 2022, in both cultivars, the  $\delta^{18}O$  seasonal patterns showed an increase during the EW formation, from early spring until late summer and a depletion in the LW, from autumn to winter. The higher  $\delta^{18}O$  values in the late EW were mainly related both to higher levels of vapor pressure deficit during periods of reduced water

availability, likely attributed to decreased  $g_s$ , and possibly access to a more enriched source of water from relatively drier, unsaturated soil profiles.

The seasonal rise in precipitation, noted from March to June 2020, would not have led to decreased  $g_s$  values and, consequently, an increase in  $\delta^{18}O$  values of leaf assimilates in both cultivars (Fig. 5). However, the generally higher  $\delta^{18}O$  values in the wood rings of Maurino were most likely associated with higher transpiration rates (Barbour, 2007). Trees might also exhibit variations in depth of root water uptake, which could potentially account for differences in  $\delta^{18}O$  values (Portarena et al., 2022), but this seems less likely in this case of study within the orchard established only few years ago.

The relationships between  $\delta^{18}O$  and  $\delta^{13}C$  observed in wood ring samples from both cultivars provide deeper insight into physiological adaptation capacity of trees.

According to the dual-isotopes conceptual model proposed by Scheidegger et al. (2000), when trees respond to environmental conditions through their stomatal behavior, this response should be reflected in a positive relationship between the  $\delta^{13}C$  and  $\delta^{18}O$  values in their plant material. This indicate that in both cultivars, changes in the  $\delta^{13}C$  values may be mainly related to variations in  $g_s$  at the leaf level, associated with soil moisture variability and evaporative demands.

Interestingly, the equation  $\delta^{18}O = 0.48 \delta^{13}C + 37$  found in Moraiolo (Fig. 5) wood branches is similar to that reported by Verheyden et al., (2004) for the wood rings of the mangrove *Rhizophora mucronata* Lam. tree species, also an evergreen tree.

The equation  $\delta^{18}O = 0.82 \delta^{13}C + 47$  found in wood rings from Maurino showed a significant steeper slope (Fig. 6). This observation aligns with the theory that a greater change in  $\delta^{18}O$  per unit change in  $\delta^{13}C$  will be found when water-vapour pressure in the intercellular spaces of leaves is higher (Barbour, 2007). A higher water vapor pressure in the intercellular spaces within plant leaves is typically associated with higher transpiration rates. In fact, when transpiration rates are high, there is a greater movement of water from the leaf's intercellular spaces into the surrounding air, leading to higher water vapor pressure within those spaces, which is reflected in further  $^{18}O$  enrichment of leaf water (Barbour, 2007).

The higher iWUE observed in Moraiolo during EW formation 2021 and 2022 are the result of either stomatal control with partial closure and/or higher rates of photosynthesis (Eilmann et al., 2010; Saurer et al., 1997; Tene et al., 2011). We suppose that, even in the drought period characterizing the late EW formation, the higher iWUE observed in Moraiolo may be related to its lower  $g_s$  and higher carboxylation capacity (Cinosi et al., 2024). In general, the higher iWUE seasonal range of variation observed in Moraiolo underlined its higher plasticity as the capacity to adjust its water-use in response to changing environmental conditions. During summer stressful condition, Moraiolo trees closed its stomata, reduced its transpiration rate and prioritized water conservation to maintain growth. This would explain the increase in  $\delta^{13}C$  in Moraiolo. In contrast, when water is abundant, it may increase  $g_s$  to optimize photosynthesis and growth, with more negative  $\delta^{13}C$  values. On the contrary, Maurino is less flexible in terms of adjusting its iWUE under different water availability conditions and remains less reactive to changing environmental conditions, with more limited variations in  $\delta^{13}C$ .

These ecophysiological distinctions are closely linked to the observed differences in aboveground development and canopy characteristics. Maurino trees exhibited a higher aboveground development, resulting in a higher leaf area index (LAI), which, in turn, leads to increased plant transpiration. This higher transpiration rate may be particularly significant during periods of elevated evapotranspiration demand. In contrast, Moraiolo trees prioritized trunk section development, less expanded crown and demonstrate a higher yield efficiency, reflecting a water-efficient strategy, conservatively allocating resources to minimize water loss.

Understanding the complexity of carbon-water allocation strategies

in olive trees and their direct influence on growth, fruit production is essential for managing crops in a world where water availability and environmental conditions are subject to ongoing changes and challenges. This knowledge can contribute to more informed decisions regarding agricultural practices and sustainable land management.

## 5. Conclusion

The findings of this research study highlighted the ecophysiological differences between Moraiolo and Maurino olive tree cultivars, shedding light on their distinct carbon-water allocation strategies in response to varying environmental conditions. Under stressful summer conditions, Moraiolo trees exhibited a capacity for water conservation by closing stomata and reducing transpiration rates while still maintaining growth. In contrast, Maurino showed less flexibility in adjusting iWUE and is comparatively less responsive to environmental fluctuations. The higher seasonal range of variation in iWUE observed in Moraiolo underscored its remarkable plasticity and ability to adjust its water-use to adapt to a changing environment.

This study shows new insight in the development of xylem and related variation in isotopic compositions in olive cultivars and enhance our understanding of the physiological mechanisms related tolerance to water-limiting and high temperature conditions and may contribute to improve olive crop management practices, enabling them to better cope with the challenges posed by a changing climate.

## Funding

This work was partially supported by the MUR-PRIN 2022, project “Varietal selection and biostimulant use in olive growing to face climate change”.

## CRediT authorship contribution statement

S.P., E.B. and F.F. conceived and designed the study. All authors performed sampling and analyses. S.P. wrote the main part of the manuscript. All authors contributed to interpretation of the overall data and wrote specific parts, made a critical revision of the whole text, and approved the submitted version of the manuscript.

## Declaration of Competing Interest

The authors declare that they have no known competing financial interests or personal relationships that could have appeared to influence the work reported in this paper.

## Data availability

Data will be made available on request.

## Acknowledgements

The authors acknowledge Luciano Spaccino and Carlotta Volterrani for their contributions to sample preparation and IRMS analyses.

## References

Anifantís, A.S., Camposo, S., Vivaldi, G.A., Santoro, F., Pascuzzi, S., 2019. Comparison of UAV photogrammetry and 3D modeling techniques with other currently used methods for estimation of the tree row volume of a super-high-density olive orchard. *Agriculture* 9 (11), 233. <https://doi.org/10.3390/agriculture9110233>.

Anselmi, C., Portarena, S., Baldacchini, C., Proietti, S., Leonardi, L., Brugnoli, E., 2022. One drop only. Easy and rapid Raman evaluation of  $\beta$ -carotene in olive oil and its relevance as an index of olive fly attack. *Food Chem.* 393, 133340 <https://doi.org/10.1016/j.foodchem.2022.133340>.

Bacelar, E.A., Moutinho-Pereira, J.M., Gonçalves, B.C., Lopes, J.I., Correia, C.M., 2009. Physiological responses of different olive genotypes to drought conditions. *Acta Physiol. Plant* 31, 611–621. <https://doi.org/10.1007/s11738-009-0272-9>.

Barbour, M.M., 2007. Stable oxygen isotope composition of plant tissue: a review. *Funct. Plant Biol.* 34, 83–94. <https://doi.org/10.1071/FP06228>.

Battipaglia, G., De Micco, V., Brand, W.A., Linke, P., Aronne, G., Saurer, M., Cherubini, P., 2010. Variations of vessel diameter and  $\delta^{13}\text{C}$  in false rings of *Arbutus unedo* L. reflect different environmental conditions. *N. Phytol.* 188 (4), 1099–1112. <https://doi.org/10.1111/j.1469-8137.2010.03443.x>.

Battipaglia, G., Saurer, M., Cherubini, P., Calfapietra, C., McCarthy, H.R., Norby, R.J., Francesca Cotrufo, M., 2013. Elevated  $\text{CO}_2$  increases tree-level intrinsic water use efficiency: insights from carbon and oxygen isotope analyses in tree rings across three forest FACE sites. *N. Phytol.* 197, 544–554. <https://doi.org/10.1111/nph.12044>.

Battipaglia, G., Campelo, F., Vieira, J., Grabner, M., De Micco, V., Nabais, C., Cherubini, P., Carrer, M., Bräuning, A., Cufar, K., Di Filippo, A., García-González, I., Koprowski, M., Klisz, M., Kirdeyanov, A.V., Zafirov, N., De Luis, M., 2016. Structure and function of intra-annual density fluctuations: mind the gaps. *Front. Plant Sci.* 7, 595. <https://doi.org/10.3389/fpls.2016.00595>.

Branquinho, S., Rolim, J., Teixeira, J.L., 2021. Climate change adaptation measures in the irrigation of a super-intensive olive orchard in the south of Portugal. *Agronomy* 11, 1658. <https://doi.org/10.3390/agronomy11081658>.

Brito, C., Dinis, L.T., Moutinho-Pereira, J., Correia, C.M., 2019. Drought stress effects and olive tree acclimation under a changing climate. *Plants* 8 (7), 232. <https://doi.org/10.3390/plants8070232>.

Brugnoli, E., Farquhar, G.D., 2000. Photosynthetic fractionation of carbon isotopes, Photosynthesis: Physiology and metabolism – advances in photosynthesis, 9. Kluwer Academic Publishers, The Netherlands, pp. 399–434R.C.LeegoodT.D.SharkeyS.von Caemmerer.

Bunn, A.G., 2008. A dendrochronology program library in R (dplR). *Dendrochronologia* 26, 115–124. <https://doi.org/10.1016/j.dendro.2008.01.002>.

Cabrera-Bosquet, L., Molero, G., Nogués, S., Araus, J.L., 2009. Water and nitrogen conditions affect the relationships of  $\Delta^{13}\text{C}$  and  $\Delta^{18}\text{O}$  to gas exchange and growth in durum wheat. *J. Exp. Bot.* 60, 1633–1644. <https://doi.org/10.1093/jxb/erp028>.

Cabrera-Bosquet, L., Albrizio, R., Nogués, S., Araus, J.L., 2011. Dual  $\Delta^{13}\text{C}/\delta^{18}\text{O}$  response to water and nitrogen availability and its relationship with yield in field-grown durum wheat. *Plant, Cell Environ.* 34, 418–433. <https://doi.org/10.1111/j.1365-3040.2010.02252.x>.

Cherubini, P., Gartner, B.L., Tognetti, R., Bräker, O.U., Schoch, W., Innes, J.L., 2003. Identification, measurement and interpretation of tree rings in woody species from mediterranean climates. *Biol. Rev.* 78, 119–148. <https://doi.org/10.1017/S1464793102006000>.

Cherubini, P., Humbel, T., Beeckman, H., Gärtner, H., Mannes, D., Pearson, C., Schoch, W., Tognetti, R., Lev-Yadun, S., 2013. Olive tree-ring problematic dating: a comparative analysis on Santorini (Greece). *PLOS ONE* 8, e54730. <https://doi.org/10.1371/journal.pone.0054730>.

Cherubini, P., Humbel, T., Beeckman, H., Gärtner, H., Mannes, D., Pearson, C., Schoch, W., Tognetti, R., Lev-Yadun, S., 2014. The olive-branch dating of the Santorini eruption. *Antiquity* 88, 267–291. <https://doi.org/10.1017/S0003598x00050365>.

Cinosi, N., Portarena, S., Almadi, L., Berrettini, A., Torres, M., Pierantozzi, P., Villa, F., Galletti, A., Famiani, F., Farinelli, D., 2023. Use of portable devices and an innovative and non-destructive index for in-field monitoring of olive fruit ripeness. *Agriculture* 13, 194. <https://doi.org/10.3390/agriculture13010194>.

Cinosi, N., Moriconi, F., Farinelli, D., Marchionni, D., Lodolini, E.M., Rosati, A., Famiani, F., 2024. Effects of summer pruning on the water status and physiology of olive trees and on fruit characteristics and oil quality. *Sci. Hortic.*, 112612 <https://doi.org/10.1016/j.scientia.2023.112612>.

Di Lena, B., Curci, G., Vergni, L., Farinelli, D., 2022. Climatic suitability of different areas in abruzzo, central italy, for the cultivation of hazelnut. *Horticulturae* 8, 580. <https://doi.org/10.3390/horticulturae8070580>.

Di Matteo, G., De Angelis, P., Brugnoli, E., Cherubini, P., Scarascia-Mugnozza, G., 2010. Tree-ring  $\Delta^{13}\text{C}$  reveals the impact of past forest management on water-use efficiency in a Mediterranean oak coppice in Tuscany (Italy), 510–510 *Ann. Sci.* 67. <https://doi.org/10.1051/forest/2010012>.

Drossopoulos, J.B., Nivais, C.A., 1988. Seasonal changes of the metabolites in the leaves, bark and xylem tissues of olive tree (*Olea europaea* L.) II. Carbohydrates. *Ann. Bot.* 62 (3), 321–327. <https://doi.org/10.1093/oxfordjournals.aob.a087664>.

Ehleringer, J.R., Monson, R., 1993. Evolutionary and ecological aspects of photosynthetic pathway variation. *Annu. Rev. Ecol. Syst.* 24, 411–439. <https://doi.org/10.1146/annurev.es.24.110193.002211>.

Eilmann, B., Buchmann, N., Siegwolf, R., Saurer, M., Cherubini, P., Rigling, A., 2010. Fast response of Scots pine to improved water availability reflected in tree-ring width and  $\delta^{13}\text{C}$ . *Plant, Cell Environ.* 33, 1351–1360. <https://doi.org/10.1111/j.1365-3040.2010.02153.x>.

Famiani, F., Cinosi, N., Paoletti, A., Farinelli, D., Rosati, A., Lodolini, E.M., 2022. Deflowering as a toll to accelerate growth of young trees in both intensive and super high density olive orchards. *Agronomy* 12, 2319. <https://doi.org/10.3390/agronomy12102319>.

Farinelli, D., Tombesi, S., 2015. Performance and oil quality of ‘Arbequina’ and four Italian olive cultivars under super high density hedgerow planting system cultivated in central Italy. *Sci. Hortic.* 192, 97–107. <https://doi.org/10.1016/j.scienta.2015.04.035>.

Farinelli, D., Boco, M., Tombesi, A., 2005. Influence of canopy density on fruit growth and flower formation. *Acta Hortic.* 247–252. <https://doi.org/10.17660/ActaHortic.2005.686.33>.

Farquhar, G.D., O’Leary, M.H., Berry, J.A., 1982. On the relationship between carbon isotope discrimination and the intercellular carbon dioxide concentration in leaves. *Funct. Plant Biol.* 9, 121–137. <https://doi.org/10.1071/pp9820121>.

- Farquhar, G.D., Ehleringer, J.R., Hubick, K.T., 1989. Carbon isotope discrimination and photosynthesis. *Annu. Rev. Plant Physiol. Plant Mol. Biol.* 40, 503–537. <https://doi.org/10.1146/annurev.pp.40.060189.002443>.
- Fernández, J.E., Perez-Martin, A., Torres-Ruiz, J.M., Cuevas, M.V., Rodriguez-Dominguez, C.M., Elsayed-Farag, S., MoralesSillero, A., García, J.M., Hernandez-Santana, V., Diaz-Espejo, A., 2013. A regulated deficit irrigation strategy for hedgerow olive orchards with high plant density. *Plant Soil* 372, 279–295.
- Gea-Izquierdo, G., Fonti, P., Cherubini, P., Martin-Benito, D., Chaar, H., Canellas, I., 2012. Xylem hydraulic adjustment and growth response of *Quercus canariensis* Willd. to climatic variability. *Tree Physiol.* 32, 401–413. <https://doi.org/10.1093/treephys/tps026>.
- Gessler, A., Ferrio, J.P., Hommel, R., Treydte, K., Werner, R.A., Monson, R.K., 2014. Stable isotopes in tree rings: towards a mechanistic understanding of isotope fractionation and mixing processes from the leaves to the wood. *Tree Physiol.* 34, 796–818. <https://doi.org/10.1093/treephys/tpu040>.
- Helle, G., Schleser, G.H., 2004. Beyond CO<sub>2</sub>-fixation by Rubisco—an interpretation of 13C/12C variations in tree rings from novel intra-seasonal studies on broad-leaf trees. *Plant, Cell Environ.* 27 (3), 367–380. <https://doi.org/10.1111/j.0016-8025.2003.01159.x>.
- Lipshitz, N., Lev-Yadun, S., 1986. Cambial activity of evergreen and seasonal dimorphics around the Mediterranean. *IAWA J.* 7, 145–153. <https://doi.org/10.1163/22941932-90000978>.
- Lodolini, E.M., Polverigiani, S., Giorgi, V., Famiani, F., Neri, D., 2023. Time and type of pruning affect tree growth and yield in high-density olive orchards. *Sci. Hortic.* 311, 111831 <https://doi.org/10.1016/j.scienta.2023.111831>.
- Portarena, S., Gavrichkova, O., Brugnoli, E., Battistelli, A., Proietti, S., Moscatello, S., Famiani, F., Tombesi, S., Zadra, C., Farinelli, D., 2022. Carbon allocation strategies and water uptake in young grafted and own-rooted hazelnut (*Corylus avellana* L.) cultivars. *Tree Physiol.* 42, 939–957. <https://doi.org/10.1093/treephys/tpab164>.
- Portarena, S., Anselmi, C., Leonardi, L., Proietti, S., Bizzarri, A.R., Brugnoli, E., Baldacchini, C., 2023. Lutein/β-carotene ratio in extra virgin olive oil: An easy and rapid quantification method by Raman spectroscopy. *Food Chem.* 404, 134748 <https://doi.org/10.1016/j.foodchem.2022.134748>.
- Roden, J.S., Farquhar, G.D., 2012. A controlled test of the dual-isotope approach for the interpretation of stable carbon and oxygen isotope ratio variation in tree rings. *Tree Physiol.* 32, 490–503. <https://doi.org/10.1093/treephys/tps019>.
- Rossi, L., Sebastiani, L., Tognetti, R., d'Andria, R., Morelli, G., Cherubini, P., 2013. Tree-ring wood anatomy and stable isotopes show structural and functional adjustments in olive trees under different water availability. *Plant Soil* 372, 567–579. <https://doi.org/10.1007/s11104-013-1759-0>.
- Saurer, M., Aellen, K., Siegwolf, R., 1997. Correlating δ13C and δ18O in cellulose of trees. *Plant, Cell Environ.* 20, 1543–1550. <https://doi.org/10.1046/j.1365-3040.1997.d01-53.x>.
- Saurer, M., Sahlstedt, E., Rinne-Garmston, K.T., Lehmann, M.M., Oettli, M., Gessler, A., Treydte, K., 2023. Progress in high-resolution isotope-ratio analysis of tree rings using laser ablation. *Tree Physiol.* 43 (5), 694–705. <https://doi.org/10.1093/treephys/tpac141>.
- Scheidegger, Y., Saurer, M., Bahn, M., Siegwolf, R., 2000. Linking stable oxygen and carbon isotopes with stomatal conductance and photosynthetic capacity: a conceptual model. *Oecologia* 125, 350–357. <https://doi.org/10.1007/s004420000466>.
- Stocker, T.F., Qin, D., Plattner, G.K., Tignor, M.M., Allen, S.K., Boschung, J., Midgley, P. M., 2014. Climate Change 2013: The physical science basis. contribution of working group I to the fifth assessment report of IPCC the intergovernmental panel on climate change., & .
- Stokes, M.A., Smiley, T.L., 1968. *An Introduction to Tree-ring Dating*. University of Arizona Press, Tucson, AZ.
- Tene, A., Tobin, B., Dyckmans, J., Ray, D., Black, K., Nieuwenhuis, M., 2011. Assessment of tree response to drought: validation of a methodology to identify and test proxies for monitoring past environmental changes in trees. *Tree Physiol.* 31 (3), 309–322. <https://doi.org/10.1093/treephys/tpq114>.
- Verheyden, A., Helle, G., Schleser, G.H., Dehairs, F., Beeckman, H., Koedam, N., 2004. Annual cyclicity in high-resolution stable carbon and oxygen isotope ratios in the wood of the mangrove tree *Rhizophora mucronata*. *Plant, Cell Environ.* 27, 1525–1536. <https://doi.org/10.1111/j.1365-3040.2004.01258.x>.
- Vinci, A., Traini, C., Portarena, S., Farinelli, D., 2023a. Assessment of the midseason crop coefficient for the evaluation of the water demand of young, grafted hazelnut trees in high-density orchards. *Water* 15, 1683. <https://doi.org/10.3390/w15091683>.
- Vinci, A., Di Lena, B., Portarena, S., Farinelli, D., 2023b. Trend analysis of different climate parameters and watering requirements for hazelnut in central Italy related to climate change. *Horticultrae* 9 (5), 593. <https://doi.org/10.3390/horticultrae9050593>.